processes

MDPI

Article

Encapsulation of Lactoferrin for Sustained Release Using Particles from Gas-Saturated Solutions

Kento Ono [1], Hiroki Sakai [1], Shinichi Tokunaga [1], Tanjina Sharmin [1,2], Taku Michael Aida [1,2] and Kenji Mishima [1,2,*]

[1] Department of Chemical Engineering, Faculty of Engineering, Fukuoka University, 8-19-1 Nanakuma Jonan-ku, Fukuoka 814-0180, Japan; td206501@cis.fukuoka-u.ac.jp (K.O.); td193008@cis.fukuoka-u.ac.jp (H.S.); td196501@cis.fukuoka-u.ac.jp (S.T.); sharmin@fukuoka-u.ac.jp (T.S.); tmaida@fukuoka-u.ac.jp (T.M.A.)

[2] Research Institute of Composite Materials, Fukuoka University, 8-19-1 Nanakuma Jonan-ku, Fukuoka 814-0180, Japan

* Correspondence: mishima@fukuoka-u.ac.jp; Tel.: +81-92-871-6631 (ext. 6428); Fax: +81-92-865-6031

Abstract: The particles from gas saturated solutions (PGSS) process were performed to encapsulate lactofer-rin, an iron-binding milk glycoprotein, using supercritical carbon dioxide ($scCO_2$). A natural en-teric polymer, shellac, was used as a coating material of lactoferrin carried out by the PGSS pro-cess. Conditions were optimized by applying different temperatures (20–50 °C) and pressures (8–10 MPa) and the particles were evaluated for particle shape and size, lactoferrin encapsulation ef-ficiency, Fourier transform infrared (FTIR) spectroscopy to confirm lactoferrin entrapment and in vitro dissolution studies at different pH values. Particles with an average diameter of 75.5 ± 7 µm were produced with encapsulation efficiency up to 71 ± 2%. Furthermore, particles that showed high stability in low pH (pH 1.2) and a sustained release over time (t_{2h} = 75%) in higher pH (pH 7.4) suggested an effective encapsulation process for the protection of lactoferrin from gastric di-gestion.

Keywords: enteric polymer; gastric digestion; PGSS; lactoferrin; shellac

Citation: Ono, K.; Sakai, H.; Tokunaga, S.; Sharmin, T.; Aida, T.M.; Mishima, K. Encapsulation of Lactoferrin for Sustained Release Using Particles from Gas-Saturated Solutions. *Processes* **2021**, *9*, 73. https://doi.org/10.3390/pr9010073

Received: 8 December 2020
Accepted: 28 December 2020
Published: 31 December 2020

1. Introduction

Lactoferrin (Lf) is an iron binding single-chain glycoprotein (MW~80 kDa, Figure 1a) which is naturally found in the milk of many mammals including humans and cows, as well as in the saliva, tears, and other secretions and in the secondary granules of neutrophils [1–5]. Lf is abundantly present in the colostrum and milk and supports new born immune defence mechanisms [6,7]. Lf also represents a powerful tool in adult host defence mechanism to stimulate the immune system and enhance the body's protection against virus and bacteria [8–10]. Most recently, a lot of attention is being paid to Lf for its in vitro antiviral activity against SARS-CoV, which is likely similar against SARS-CoV-2 as both viruses depend on the same angiotensin-converting enzyme 2 (ACE2) receptor for cell entry [8]. Other physiological functions of Lf involve preventing tissue damage related to aging, promoting healthy intestinal bacteria [11], maintaining vaginal acidity by promoting growth of selected strains of probiotics [12], preventing cancer, etc. [13]. However, low availability during development and aging, Lf is often taken as an oral supplement. In infants, Lf survives gastric digestion because of the immature state of the neonatal gastrointestinal system, however, Lf is rapidly digested in the adult stomach due to enzymatic hydrolysis and fails to reach the Lf receptors (hLfRs) present in the small intestine. Therefore, protecting Lf from the gastric acidic environment and ensuring its delivery to the targeted site is a crucial issue.

Microencapsulation is one of the promising techniques in protecting functional ingredients in food, cosmetic and pharmaceutical applications. Several encapsulation technologies have been developed for the encapsulation of Lf such as calcium-alginate nanospheres via

emulsification [14], or multilayer microcapsules via Layer-by-Layer assembly of bovine serum albumin and tanic acid [15]. However, alginate is sensitive to gastric acid which causes alginate to precipitate leading to pre-mature release of Lf which is supposed to be released in the intestine. On the other hand, the amount of Lf absorbed by $CaCO_3$ particles is significantly low in multilayer capsules composed of Lf in bovine serum albumin and tannic acid, performed through absorption of Lf by porous $CaCO_3$ microparticles. Therefore, a more effective encapsulation technique needs to be designed for optimal delivery across the gastro-intestinal route that not only protects Lf from enzymatic degradation but also enables sustained release to the targeted area.

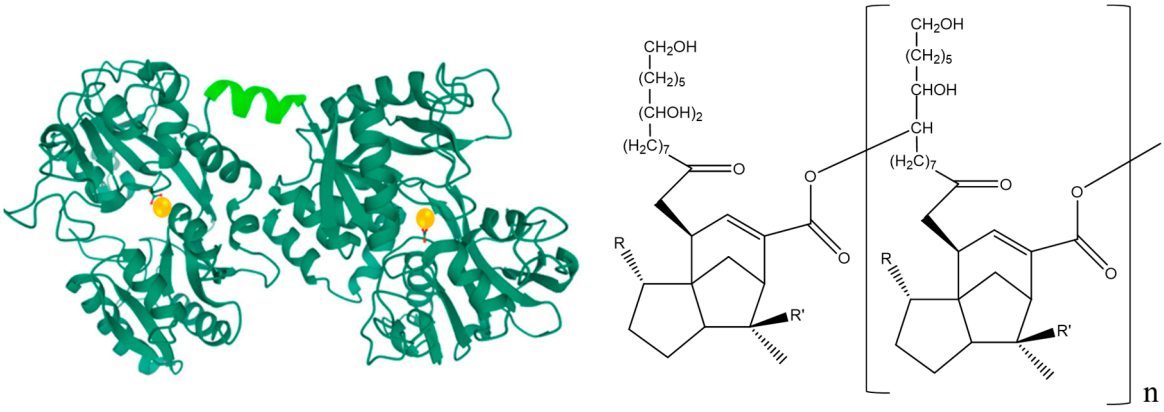

(**a**) (**b**)

Figure 1. (**a**) Crystal structure of diferric bovine lactoferrin, Lf, MW ~80 kDa (PDB entry 1BLF). The N-lobe and C-lobe connecting α-helix is highlighted in light green (aa. 334–344), and the ferric irons are depicted as orange spheres; and (**b**) Chemical structure of shellac, MW ~586.7 g/mol.

In this work, Lf encapsulation initiated with an alternative encapsulation technology, particles from gas saturated solutions (PGSS) process, based on the use of supercritical carbon dioxide ($scCO_2$). By this technique, a gas saturated solution of the coating material is expanded through a nozzle. This sudden depressurization promotes the rapid vaporization of the gas dissolved, that together with the intense cooling due to the Joule-Thomson effect that promotes CO_2 expansion [16], enhances encapsulated particle formation. Shellac, a kind of resin secreted by the female lac bug on trees in the forests of southeastern Asia, is used in this work as a coating material. The chemical structure of shellac is shown in Figure 1b. Shellac is widely used in colon drug delivery system (DDS) as a natural enteric polymer because it cannot be dissolved with gastric acid [17].

Therefore, the aim of this work was to study the encapsulation of Lf with shellac using particles from gas-saturated solutions (PGSS) process: first, conditions were optimized by applying different temperatures (20–50 °C) and pressures (8–10 MPa) and the particles shape, size and encapsulation efficiency were evaluated; and second, the in vitro studies of dissolution of Lf encapsulated in shellac microcapsules at different pH values were studied with the aim to evaluate the sustained release.

2. Methods

2.1. Materials

Lactoferrin, from bovine milk (>95.0 wt%, Iron (Fe) 0.005–0.035 wt%, FUJIFILM Wako Pure Chemical Co, Ltd., Osaka, Japan), liquid Shellac (Shellac 10%, Ethanol 90%), CO_2 (>99.9 vol.%, Fukuoka Sanso Co., Ltd., Fukuoka, Japan), were purchased and used as received without further purification.

2.2. Preparation of Shellac Microcapsules of Lactoferrin

The process flow diagram of the PGSS apparatus equipped with a high-pressure cell (inner volume of 500 cm^3, SCV500A, Akico Co., Tokyo, Japan) used to produce microcapsules of Lf is shown in Figure 2. At first, 0.2 g of Lf and 10 mL of shellac was loaded into the pre-heated high-pressure stirred cell (max. 940 rpm) and sealed. The high-pressure autoclave was kept under desired temperature (from 20 to 50 °C). CO_2 was loaded into the high-pressure autoclave to the desired pressure and mixed extensively for 5 min with the pre-loaded materials to form CO_2 saturated solution. CO_2 saturated solution was then charged through outer tube by opening valve V4 and expanded into a chamber with water (100 mL) at atmospheric pressure leading to the formation of microcapsules by precipitation. The recovered microcapsules were separated from water using centrifugation (10 min, 4000 rpm). The concentration of uncoated Lf dissolved in the water was measured by a UV-vis spectrophotometer at 266 nm. Encapsulation efficiency (EE%) was expressed by the following Equation (1).

$$\text{Encapsulation efficiency (\%)} = (W_1 - W_2)/W_1 \times 100 \quad (1)$$

The difference between the amount of loaded Lf in initial loading solution before encapsulation (W1) and the amount of uncoated Lf remained in supernatant after centrifugation (W2) divided by initial protein concentration is equivalent to the encapsulation efficiency (Equation (1)).

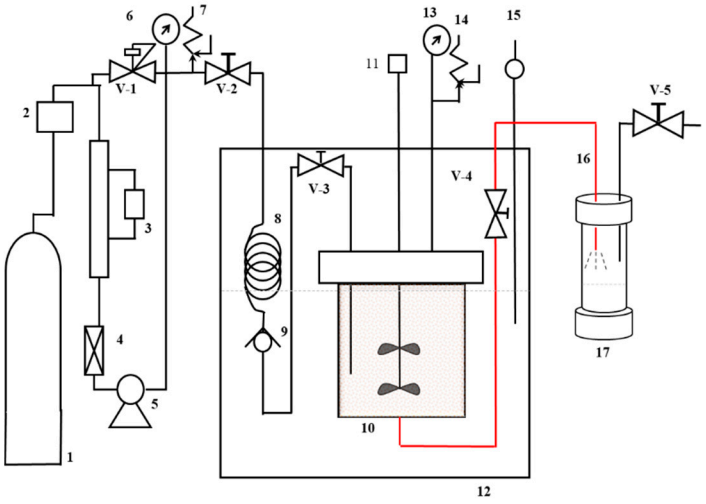

Figure 2. Schematic diagram of apparatus used in PGSS process. 1: gas cylinder, 2: dryer, 3: cooling unit, 4: filter, 5: pump, 6: pressure gauge, 7: safety valve, 8: preheater, 9: check valve, 10: high-pressure cell, 11: agitator, 12: water bath, 13: pressure gauge, 14: safety valve, 15: thermometer, 16: depressurization tunnel, and 17: atmospheric collector vessel with water. V-1 indicates a back-pressure regulator, and V-2 to 5: stop valves.

2.3. Study of Microcapsule Morphology and Size Distribution

The structure and morphology of the products were analyzed before and after the PGSS process using a scanning electron microscope (SEM, JEOL JSM6060) and the particle size were investigated by using laser diffraction particle size analyzer (SALD-2000). The release studies of Lf from shellac microcapsules were measured via a UV-vis spectrophotometer (JASCO, V-550, Tokyo, Japan). Fourier transform infrared (FTIR) spectra of pure components, and the shellac microcapsules of Lf were recorded via attenuated total reflectance FTIR spectrometer (FT/IR-4600, JASCO, Tokyo, Japan), and infrared measurements were performed in transmission in the scanning range of 500–4000 cm^{-1} at room temperature.

2.4. Lf microcapsule In Vitro Release

The sustained release rate of Lf from shellac microcapsules was investigated via in vitro release study using vertical Franz-type diffusion cells (VIDTEK, Iwaki, Fukuoka, Japan) for 2 h in simulated gastric fluid (SGF) of pH 1.2 (representing stomach pH) followed by simulated intestinal fluid (SIF) of pH 7.4 (representing small intestine pH) for 6 h. A hydrophilic PTFE membrane (0.45 um pore size, thickness 65 µm, 47 mm diameter; Merck Millipore, Tokyo, Japan) was placed between the upper donor chamber and the receptor chamber of the diffusion cell. SGF of pH 1.2 was prepared by adding 2 g of NaCl and 7 mL of HCl in sufficient MilliQ water to make 1000 mL. SIF of phosphate buffer of pH 7.4 was prepared by dissolving 8 g of NaCl, 0.2 g of KCl, 1.44 g of Na_2HPO_4 and 0.24 g of KH_2PO_4 in 800 mL of MilliQ water followed by adjusting the pH to 7.4 with HCl and adding sufficient MilliQ water to make 1000 mL. Exactly 10 mg of shellac microcapsules was placed on the membrane and filled up the receptor chamber with SGF followed by SIG as required wetting the membrane and the microparticles. The top plate was tightly sealed to avoid evaporation. At fixed intervals (0–480 min.), samples of release liquid were drawn and, the UV absorbance of the microcapsule release medium was measured at 266 nm with a UV-vis detector (JASCO, V-550, Tokyo, Japan). The release medium was returned back to the receptor chamber after measurement.

2.5. Statistical Analysis

All analyses were performed in triplicate. The data were analyzed by one-way analysis of variance (ANOVA) accompanied by Turkey's post hoc. The level of significance was set at $p < 0.05$.

3. Results and Discussion

3.1. Encapsulation of Lf in Shellac by PGSS

Lf encapsulation in shellac by the PGSS process was studied using varying pre-expansion pressures (8–10 MPa) and pre-expansion temperatures (20–50 °C). Figure 3a,b provides the SEM imaged of crude Lf and Lf encapsulated shellac microcapsules produced by PGSS process of $scCO_2$ solutions at 40 °C and 10 MPa, and Figure 3c provides the particle size distribution (PSD) of the Lf encapsulated shellac microcapsules at 10 MPa and 40 °C. As shown in Figure 4, produced particles displayed very similar morphology with irregular shapes which is a very common feature in PGSS.

Table 1 presents a summary of the experimental conditions tested together with PSD and encapsulation efficiency (EE%). As shown in Table 1, Lf encapsulated in shellac microcapsules successfully produced at different pre-expansion pressures (8–10 MPa) and 40 °C pre-expansion temperature. At this condition, the particle size was significantly reduced as the pressure increased from 8 to 10 MPa from 143.0 ± 4 to 75.4 ± 7, respectively, with relatively narrow particle size distributions ($d_{0.1}$ = 61.8 to 36.8 µm and $d_{0.9}$ = 338.5 to 161.3 µm, respectively). This trend can be related to the increase of the solubility of $scCO_2$ in the polymer, which increases as pre-expansion pressure is increased [18]. Polymer plasticity increases with a higher amount of CO_2 dissolved into the polymer at a higher pre-expansion pressure, the Joule-Thomsone effect produced by the release of CO_2 from the polymer during the expansion is stronger, which produces significantly reduced particle size. It can also be seen that encapsulation efficiency increased from 51 ± 5% to 71 ± 2% when expansion pressure increased from 8 to 10 MPa, respectively at 40 °C. However, the solubility of CO_2 into the polymer decreased at lower temperatures (20 and 30 °C). This may occur because of the lower saturation power of CO_2 in liquid (at 20 °C) or sub-critical (30 °C) conditions and caused polymer particles to precipitate and thereby, aggregated inside the high-pressure cell upon depressurization (Figure S1a,b). On the other hand, particle agglomeration was also noted at higher temperatures (i.e., 50 °C, Figure S1c) which may be attributed to the susceptibility of Lf molecules to higher temperature [19] as fine particles were successfully produced using only shellac (without Lf) at higher temperatures (50 °C, Figure S1d).

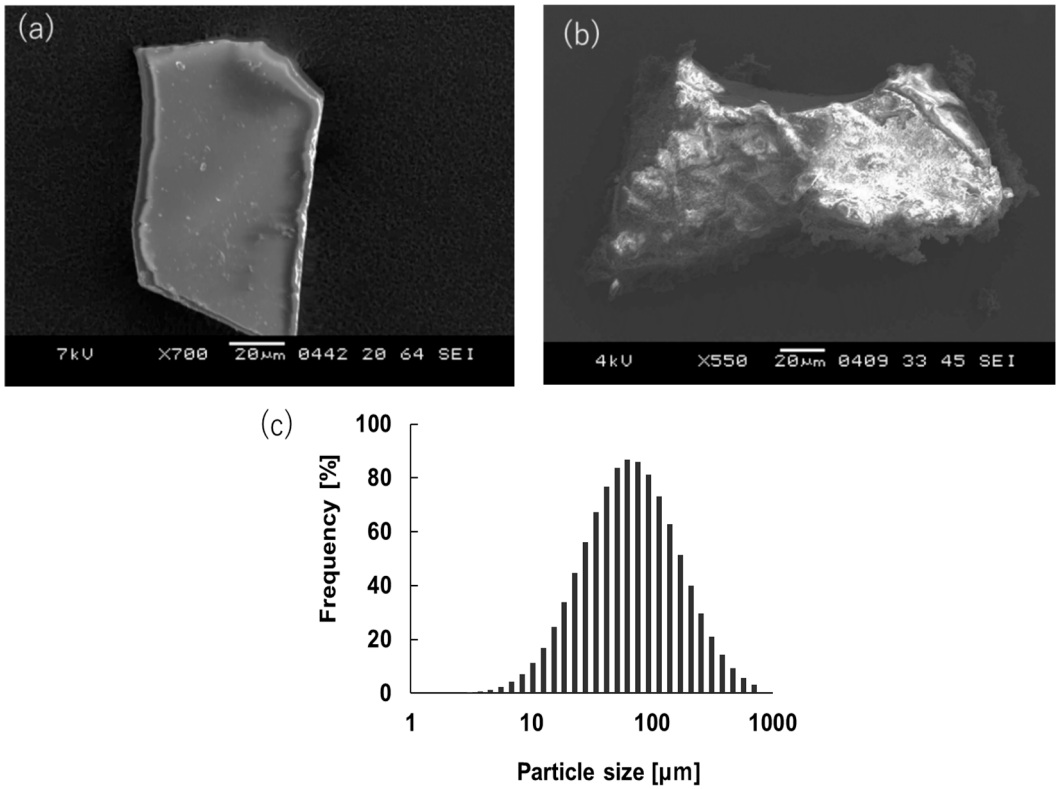

Figure 3. SEM images of (**a**) crude Lf; (**b**) Lf encapsulated shellac microcapsules produced by PGSS process of $scCO_2$ solutions at 40 °C and 10 MPa. (**c**) Particle size distribution of the Lf encapsulated shellac microcapsules produced by PGSS process of $scCO_2$ solutions at 40 °C and 10 MPa.

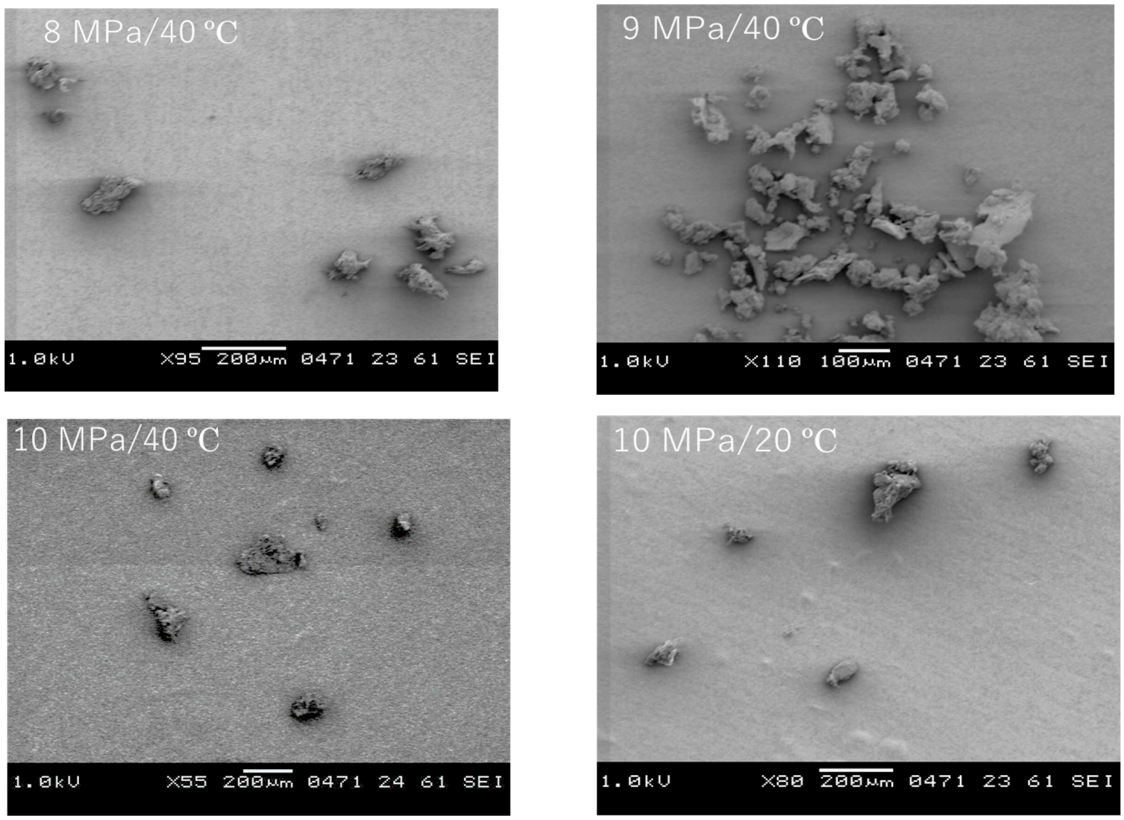

Figure 4. *Cont.*

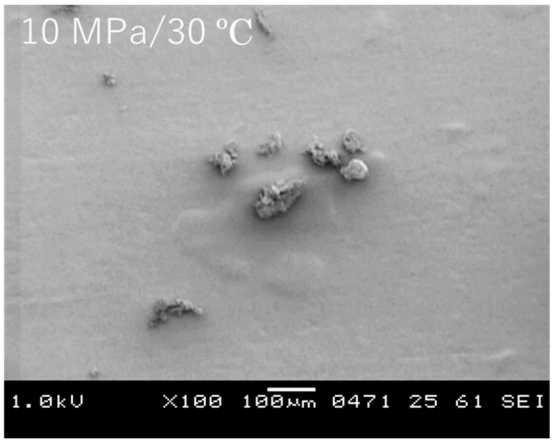

Figure 4. Morphology of Lf loaded shellac microparticles produced at different P and T conditions of supercritical CO_2 in the PGSS process.

Table 1. Influence of process parameters on particle size distribution and encapsulation efficiency of Lf microcapsules.

Experimental Conditions				Avg. Particle Size [µm]	Particle Size Distribution (PSD)				EE [%]
P [MPa]	*T* [°C]	Lactoferrin [g]	Shellac EtOH Ratio		$d_{0.1}$	$d_{0.5}$	$d_{0.9}$	Span	
8	40	0.2	1:10	143.0 ± 4^{b}	61.8	144.3	338.5	1.91	51 ± 5^{a}
9	40	0.2	1:10	132.6 ± 10^{b}	39.8	153.0	592.0	3.61	
10	40	0.2	1:10	75.4 ± 7^{a}	36.8	77.2	161.3	1.61	71 ± 2^{b}
10	50	0.2	1:10	Agglomerated	-	-	-	-	-
10	30	0.2	1:10	59.8 ± 2^{a}	5.09	59.9	559.8	9.92	-
10	20	0.2	1:10	71.4 ± 3^{a}	12.17	77.56	423.3	5.30	-

Here, $d_{0.5}$ refers to the median particle size; whereas $d_{0.1}$ and $d_{0.9}$ refer to the maximum particle diameter below which 10% and 90% of the sample volume exists, respectively; Span = $d_{0.9} - d_{0.1}/d_{0.5}$. Mean values in the same column with different letters are significantly different at $p < 0.05$.

3.2. Fourier Transform Infra-Red Spectroscopy (FT-IR) Analysis

FT-IR analysis was conducted to confirm the entrapment of Lf in the shellac microparticles produced by PGSS process of $scCO_2$ solutions at 40 °C and 10 MPa. Figure 5 presents the FTIR spectra of Lf, shellac, and Lf encapsulated shellac microcapsules. The FTIR spectra of Lf (Figure 5a) showed the stretching and bending vibrations of amide I (1637 cm^{-1}), amide II (1528 cm^{-1}), and C-O-C stretch (1073 cm^{-1}) which are the major characteristics of Lf and sensitive to secondary structure.

The amide I is more commonly used for characterizing the secondary structure and is due to C=O stretching vibrations of the peptide bonds, which are modulated by the secondary structure (α-helix, β-sheet, etc.). The same pattern of stretching frequencies for amide I (1637 cm^{-1}), and amide II (1528 cm^{-1}) were observed in the same position in the shellac microparticles (Figure 5c) suggesting that there was no shift in stretching frequency between Lf and shellac microcapsules. FTIR spectra of shellac (Figure 5b) showed strong symmetric and asymmetric stretching vibrations of CH_2 at 2855 cm^{-1} and 2927 cm^{-1}, respectively. The other strong vibrations peaked at 1710 cm^{-1} are attributed to the C=O stretching vibration of esters. The large band in the range 3100–3600 cm^{-1} with a maximum at about 3428 cm^{-1} is attributed to the O–H stretching vibration, while the O–H bending vibration is identified at 1250 cm^{-1}. The absorption bands at 1167 and 1042 cm^{-1} are due to stretching vibrations of C–O and C–C bonds. The characteristic peaks of shellac in microparticles can be observed at 2927 cm^{-1}, 2855 cm^{-1}, 1710 cm^{-1}, and 1167 cm^{-1} (Figure 5c). Therefore, as the shellac microcapsules exhibited characteristic peaks of both Lf (amide I and II at 1637 cm^{-1} and 1528 cm^{-1}, respectively) and shellac (C=O at 1710 cm^{-1} and CH_2 at 2855 cm^{-1} and 2927 cm^{-1}), suggesting successful encapsulation of Lf without any interaction within the polymer.

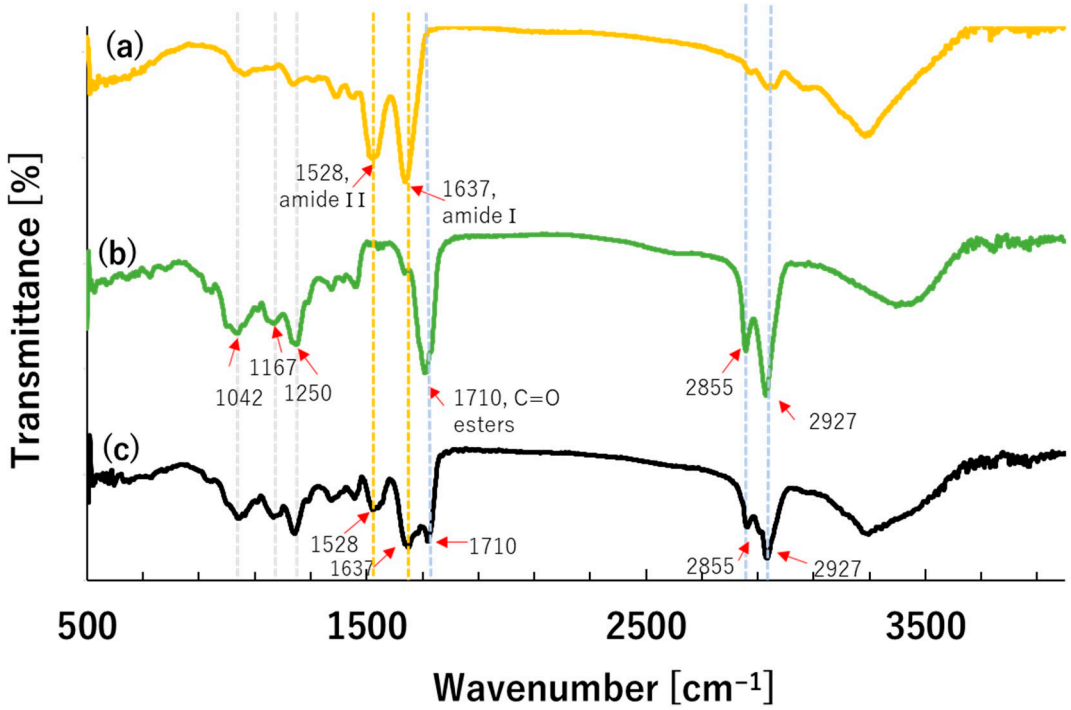

Figure 5. FTIR spectra of (**a**) crude Lf; (**b**) shellac and (**c**) Lf encapsulated shellac microcapsules produced by PGSS process of $scCO_2$ solutions at 40 °C and 10 MPa.

3.3. In Vitro Release

The sustained release profiles of Lf from shellac microcapsules in SGF (pH 1.2) followed by SIF (pH 7.4) are shown in Figure 6. The microcapsules provided a persistent behavior in SGF environment with a very small percentage of Lf release, not more than 11% over time (120 min) establishing that the shellac microcapsules have acidic environment-resistant characteristics. On the other hand, a biphasic Lf release was recorded in the SIF environment: an initial rapid Lf release phase (73% burst in 50 min) was followed by the slow and prolonged phase. The initial burst effect which is frequently observed in protein loaded microparticles because of their high solubility [20] was successfully delayed by the encapsulation of Lf in shellac microcapsules produced by PGSS. The highly hydrophobic nature of shellac in aqueous solution can be attributed to the delayed release observed in the shellac microcapsules. The third-slower release phase was thought to involve the diffusion of Lf entrapped within the inner part of the shellac matrix by means of ester channels of a network of pores. Furthermore, the burst effect may be favorable because a high initial release produces an instant effect which can be subsequently maintained for a prolonged period by a sustained release.

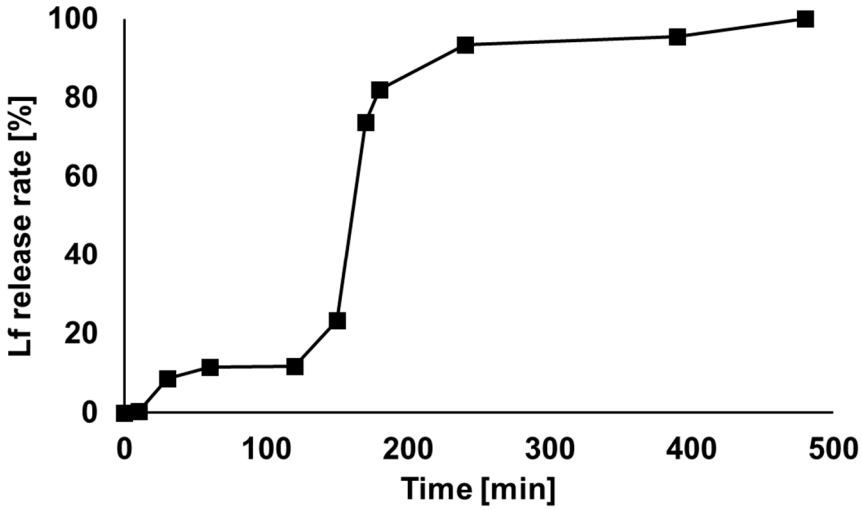

Figure 6. Sustained release profiles of Lf from shellac microcapsules produced by PGSS process of $scCO_2$ solutions at 40 °C and 10 MPa in simulated gastric fluid (SGF) (0–120 min in pH 1.2) followed by simulated intestinal fluid (SIF) (120–480 min in pH 7.4).

4. Conclusions

Sustained release Lf microcapsules were successfully prepared by PGSS process using natural enteric polymer shellac which can remain in the stomach for a long time. Particles produced at 40 °C and 10 MPa showed the highest encapsulation efficiency (71 ± 2%). In vitro release study revealed that shellac coated Lf microcapsules could be resistant against acidic environment, and they would rapidly release Lf under mild alkali conditions with an initial high followed by the slow and prolonged phase release. It could be concluded that shellac coated Lf microcapsules could be a good way to enhance the stability and sustained release of Lf favorable for targeting colon-specific drug delivery system. This study provides the basis for the application of shellac as a potential sustained drug delivery vehicle.

Supplementary Materials: The following are available online at https://www.mdpi.com/2227-9717/9/1/73/s1, Figure S1. Images of Lf loaded shellac microparticle-agglomeration by PGSS process at (a) 20 °C, (b) 30 °C, and (c) 50 °C, at 10 MPa. SEM images of shellac (sole) microparticles produced by PGSS process at 10 MPa and at 50 °C (d).

Author Contributions: Conceptualization, T.S., T.M.A. and K.M.; Data curation, K.O.; Formal analysis, K.O. and H.S.; Funding acquisition, K.M.; Investigation, K.O.; Methodology, K.O.; Project administration, K.M.; Resources, K.O., H.S. and S.T.; Software, K.O. and H.S.; Supervision, K.M.; Validation, K.O., H.S. and S.T.; Visualization, K.O. and H.S.; Writing—original draft, K.O.; Writing—review & editing, T.S., T.M.A. and K.M. All authors have read and agreed to the published version of the manuscript.

Funding: This work was funded by JSPS KAKENHI Grant Number 17K06899.

Institutional Review Board Statement: Not applicable.

Informed Consent Statement: Not applicable.

Data Availability Statement: No new data were created or analyzed in this study. Data sharing is not applicable to this article.

Conflicts of Interest: The authors declare no conflict of interest.

References

1. Gonzalez-Chavez, S.A.; Arevalo-Gallegos, S.; Rascon-Cruz, Q. Lactoferrin: Structure, function and applications. *Int. J. Antimicrob. Agents* **2009**, *33*, 301–308. [CrossRef] [PubMed]
2. Albar, A.H.; Almehdar, H.A.; Uversky, V.N.; Redwan, E.M. Structural heterogeneity and multifunctionality of lactoferrin. *Curr. Protein Pept. Sci* **2014**, *15*, 778–797. [CrossRef] [PubMed]
3. Park, Y.W.; Nam, M.S. Bioactive Peptides in Milk and Dairy Products: A Review. *Korean J. Food Sci. Anim. Resour.* **2015**, *35*, 831–840. [CrossRef] [PubMed]
4. Vogel, H.J. Lactoferrin, a bird's eye view. *Biochem. Cell Biol.* **2012**, *90*, 233–244. [CrossRef] [PubMed]
5. Giansanti, F.; Panella, G.; Leboe, L.; Antonini, G. Lactoferrin from Milk: Nutraceutical and Pharmacological Properties. *Pharmaceuticals* **2016**, *9*, 61. [CrossRef] [PubMed]
6. Sánchez, L.; Calvo, M.; Brock, J.H. Biological role of lactoferrin. *Arch. Dis. Child.* **1992**, *67*, 657–661. [CrossRef] [PubMed]
7. Brock, J. Lactoferrin in human milk: Its role in iron absorption and protection against enteric infection in the newborn infant. *Arch. Dis. Child.* **1980**, *55*, 417–421. [CrossRef] [PubMed]
8. Kell, D.B.; Heyden, E.L.; Pretorius, E. The Biology of Lactoferrin, an Iron-Binding Protein That Can Help Defend Against Viruses and Bacteria. *Front. Immunol.* **2020**, *11*, 1221. [CrossRef] [PubMed]
9. Chang, R.; Ng, T.B.; Sun, W.-Z. Lactoferrin as potential preventative and adjunct treatment for COVID-19. *Int. J. Antimicrob. Agents* **2020**, *56*, 106118. [CrossRef] [PubMed]
10. Valenti, P.; Antonini, G. Lactoferrin: An important host defence against microbial and viral attack. *Cell. Mol. Life Sci.* **2005**, *62*, 2576–2587. [CrossRef] [PubMed]
11. Vega-Bautista, A.; Garza de la, M.; Carrero, J.C.; Campos-Rodríguez, R.; Godínez-Victoria, M.; Drago-Serrano, M.E. The Impact of Lactoferrin on the Growth of Intestinal Inhabitant Bacteria. *Int. J. Mol. Sci.* **2019**, *20*, 4707. [CrossRef] [PubMed]
12. Valenti, P.; Rosa, L.; Capobianco, D.; Lepanto, M.S.; Schiavi, E.; Cutone, A.; Paesano, R.; Mastromarino, P. Role of Lactobacilli and Lactoferrin in the Mucosal Cervicovaginal Defense. *Front. Immunol.* **2018**, *9*, 376. [CrossRef] [PubMed]
13. Yoo, Y.C.; Watanabe, R.; Koike, Y.; Mitobe, M.; Shimazaki, K.; Watanabe, S.; Azuma, I. Apoptosis in human leukemic cells induced by lactoferricin, a bovine milk protein-derived peptide: Involvement of reactive oxygen species. *Biochem. Biophys. Res. Commun.* **1997**, *237*, 624–628. [CrossRef] [PubMed]
14. De Etchepare, M.A.; Barin, J.S.; Cichoski, A.J.; Jacob-Lopes, E.; Wagner, R.; Fries, L.L.M.; Menezes, C.R. Microencapsulation of probiotics using sodium alginate. *Ciência Rural* **2015**, *45*, 1319–1326. [CrossRef]
15. Kilic, E.; Novoselova, M.; Lim, S.; Pyataev, N.; Pinyaev, S.; Kulikov, O.; Sindeeva, O.; Mayorova, O.; Murney, R.; Antipina, M.; et al. Formulation for Oral Delivery of Lactoferrin Based on Bovine Serum Albumin and Tannic Acid Multilayer Microcapsules. *Sci. Rep.* **2017**, *7*, 44159. [CrossRef] [PubMed]
16. Mishima, K. Biodegradable particle formation for drug and gene delivery using supercritical fluid and dense gas. *Adv. Drug Deliv. Rev.* **2008**, *60*, 411–432. [CrossRef] [PubMed]
17. Limmatvapirat, S.; Panchapornpon, D.; Limmatvapirat, C.; Nunthanid, J.; Luangtana-Anan, M.; Puttipipatkhachorn, S. Formation of shellac succinate having improved enteric film properties through dry media reaction. *Eur. J. Pharm. Biopharm.* **2008**, *70*, 335–344. [CrossRef] [PubMed]
18. Labuschagne, P.W.; Naicker, B.; Kalombo, L. Micronization, characterization and in-vitro dissolution of shellac from PGSS supercritical CO_2 technique. *Int. J. Pharm.* **2016**, *499*, 205–216. [CrossRef] [PubMed]
19. Brisson, G.; Britten, M.; Pouliot, Y. Heat-induced aggregation of bovine lactoferrin at neutral pH: Effect of iron saturation. *Int. Dairy J.* **2007**, *17*, 617–624. [CrossRef]
20. White, L.J.; Kirby, G.T.; Cox, H.C.; Qodratnama, R.; Qutachi, O.; Rose, F.R.; Shakesheff, K.M. Accelerating protein release from microparticles for regenerative medicine applications. *Mater. Sci. Eng. C Mater. Biol. Appl.* **2013**, *33*, 2578–2583. [CrossRef] [PubMed]